A Speed-up Method for Numerical Simulations of Multi-strokes Cold Metallic Sheet Forming Processes

Anouar Krairi, Jalil Marmi, Sabrina Gastebois, Mark Veldhuis, Matthäus Kott

Available online at www.sciencedirect.com

ScienceDirect

Procedia Manufacturing 00 (2019) 000–000

Procedia MANUFACTURING

www.elsevier.com/locate/procedia

23rd International Conference on Material Forming (ESAFORM 2020)

A Speed-up Method for Numerical Simulations of Multi-strokes Cold Metallic Sheet Forming Processes

Anouar Krairi[a, *], Jalil Marmi[a], Sabrina Gastebois[b], Mark Veldhuis[c], Matthäus Kott[d]

[a]*Materials innovation institute (M2i), Van der Burghweg 1, 2628 CS DELFT, The Netherlands*
[b]*ESI Group, EXCELCAR - La Janais, Route de Nantes, BP 57633, 35176, Chartres-de-Bretagne, France*
[c]*Philips, High Tech Campus 5, 5656AE, Eindhoven, The Netherlands*
[d]*Opel Automobile GmbH, Bahnhofplatz 1, 65423 Rüsselsheim, Germany*

* Corresponding author. Tel.: +31 6 285 6730; fax: +31 15 278 9236. *E-mail address:* a.krairi@M2i.nl

Abstract

The numerical simulation of multi-strokes sheet metal cold forming is very CPU time consuming especially if all relevant physical phenomena are considered. For a single stroke FE simulation, although the process is cold forming, thermo-mechanical coupling should be taken into account. Moreover, friction between the blank and the tools should be correctly modeled. If such complexity is included for the simulation of a single stroke in cold forming, simulating multi-strokes process and maybe multi-steps cold metallic sheet forming, will be extremely CPU time consuming and even unrealistic to be performed. In this work, the authors propose a speed-up method called "jump in strokes method", which allows a CPU reduction up to 60%. This method was applied for two industrial use cases: the first one was proposed by Philips representing small parts used in shavers and the second one by Opel representing the production of large panels in automotive industry.

Keywords: Numerical Simulation; Speed-up; Multiple strokes; Ssheet Metal Forming; Friction; Warm-up

1. Introduction

The cold forming process is commonly used in different industries at high production rates, which leads to important heat generation originated by the mechanical dissipated energy during the forming of the metallic sheet. This heat influences the behavior of the tools and their friction with the blank. As a result, the final product shape quality is only stable during the steady state, when the temperature field in the tools are relatively constant. This is known as the start-up effect. Generally, trial and error methods are employed to reach the desired product shape quality. Since, this method is time-consuming, numerical simulation of the start-up effect and prediction of the final product quality at steady state, is one of the main objectives of the ASPECT (Advanced Simulation and control of tribology in metallic forming Processes for the North-West European Consumer goods and Transport sectors) project. Advanced FE models were developed taking into account the effect of temperature on the friction between the metallic sheet and the tools, allowing to estimate the shape and the quality of the final product after experiencing large deformations. These models allow the simulation of a single stroke of the forming process. For multiple strokes, given the complexity of the FE models and the high computation time for one stroke, the full simulation of a real industrial part until reaching the steady state is not possible. Therefore, a speed-up method was developed by M2i and ESI, and implemented using two different FE commercial software. It's a method based on extrapolation, it was initially used in fatigue damage computations in which a lot of cycles of simulations are needed [1]. The proposed method, called jump in strokes, allows a CPU reduction up to 60%. This method was applied for two industrial use cases: the first use-case was

proposed by the Philips (small parts) and the second by Opel (large panels). In this paper, the authors will present the proposed jump in strokes method and its application for the two use cases.

In the first section, the theory and main assumptions behind the jump-in-strokes method are presented. In the next sections, the method is applied for the two use cases. For each application a full description is provided and the FE model for a single stroke is described. Implementation of the jump in strokes method within the FE software is detailed: MSC.Marc for the first application and ESI PAM-STAMP [2] for the second application.

2. Theory and assumptions

The proposed method is based on an approximation of the nodal temperature (T) of the tools by a second order Taylor expansion. Given an initial series of simulations corresponding to a minimum of 3 strokes, the Taylor development of the temperature after a jump in strokes Δt, is developed around the stroke at the middle of the current FE computed group of strokes by:

$$T(t+\Delta t) = T(t) + \frac{\mathrm{dT(t)}}{dt}\Delta t + \frac{\mathrm{d^2T(t)}}{dt^2}\frac{\Delta t^2}{2} + o(\Delta t^3) \quad (1)$$

An illustration of the method is given in the Fig. 1.

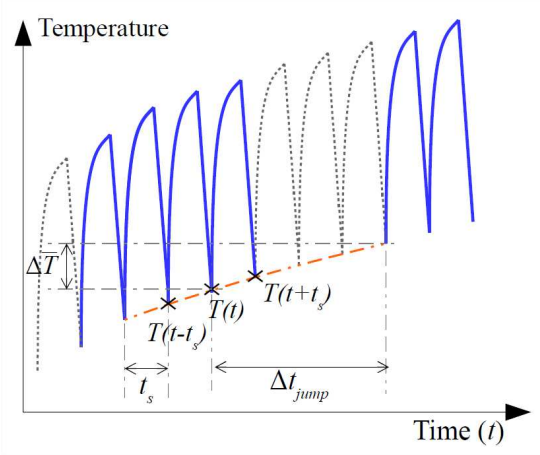

Fig. 1: Scheme of the Jump in strokes method.

A first series of incremental strokes are computed FEM. Its number must be at least equal to three because of the use of the centered scheme (see Fig. 1). In general, the higher the number of simulated strokes, the better is the accuracy of the predictions. The number of simulated strokes between jumps is taken equal to four in this work, to increase the stability of the method and limit the total computational time.

Firstly, the maximum temperature increase per jump is denoted $\Delta\bar{T}$, which may be defined by the user or may be also computed from the initial series of strokes. It is only computed or imposed once before the first jump.

The approximation of first and second order time derivative of the nodal temperatures are computed using the central difference scheme, as given in equation 2:

$$\begin{cases} \frac{dT_i(t)}{dt} = & \frac{|T_i(t+t_s)-T_i(t-t_s)|}{2t_s} \\ \frac{d^2T_i(t)}{dt^2} = & \frac{T_i(t+t_s)-2T_i(t)+T_i(t-t_s)}{{t_s}^2} \end{cases} \quad (2)$$

Given the increase of temperature $\Delta\bar{T}$ and the maximum first derivative of nodal temperature, the time for the jump $(\Delta t_{\mathrm{jump}})$ which corresponds to several non-simulated strokes, is computed as:

$$\Delta t_{jump} = \frac{\Delta\bar{T}}{\max\limits_{i=1,\dots,N}\left(\left|\frac{dT_i(t)}{dt}\right|\right)} \quad (3)$$

Finally, the temperature field in the tools is extrapolated using the Taylor expansion taking the intermediate simulated stroke temperature field as reference:

$For\ i = 1..,N$:

$$T_i(t+\Delta t_{jump}) = T_i(t) + \frac{dT_i(t)}{dt}\Delta t_{jump} + \frac{d^2T_i(t)}{dt^2}\frac{{\Delta t_{jump}}^2}{2} \quad (4)$$

3. Application to consumer goods

3.1. The Philips use case

The Philips use case is selected to represent consumer goods products such as shavers. It is a two-step drawing process that leads to the product shown in Fig. 2. The process, as schematically shown in Fig. 3, starts with a blank of 29.5 mm diameter and 0.3 mm thickness including a 2 mm diameter central hole. The blank material is AISI420 in annealed state. It consists of deep-drawing in a first step and redrawing in a second step.

Fig. 2: Final product of the Philips use case.

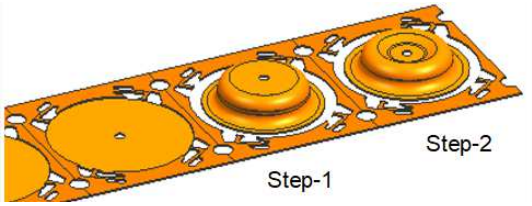

Fig. 3: Schematic overview of the two drawing steps to create the Philips demonstrator.

3.2. The finite element model for a single stroke

In this section, we describe the finite element model used to simulate Philips' deep drawing use case: Geometry and mesh, behavior laws, temperature dependent friction model.

Geometry and mesh: the tools (blank holder, punch, die and ejector) and blank are represented. The two steps are described

by axisymmetric FE models in the FE software MSC.Marc, using fully meshed tools, which allow to capture their temperature distribution. Both the tools and the blank are modelled as deformable bodies.

Fig. 4 shows the geometry and the mesh of the tools and the blank for the first and the second step. The shape of the blank after each step is also showed. The blank geometry and its state variables (including the temperature field) are transferred from the step-1 model to the step-2 model using the so-called section file in MSC.Marc.

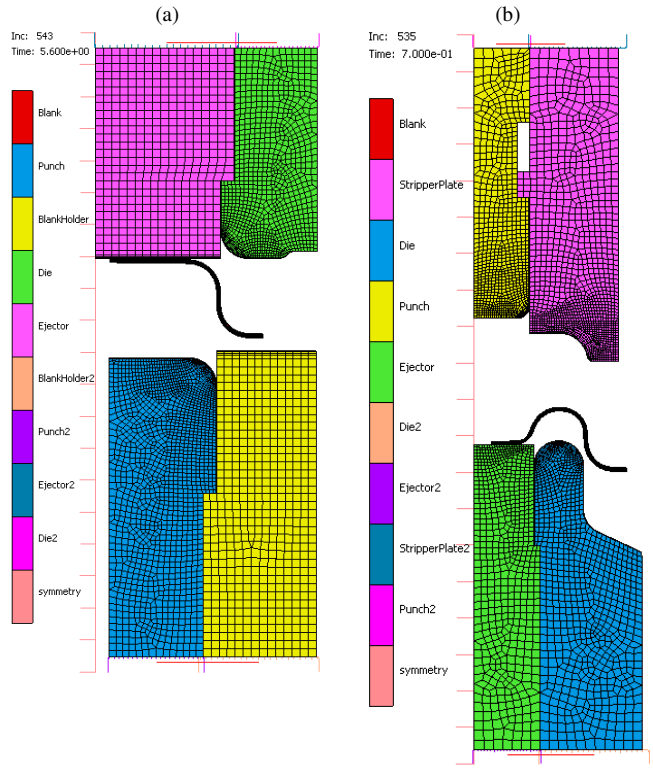

Fig. 4: (a) First (deep drawing) step with meshed deformable tools. (b) Second (redrawing) step with meshed deformable tools.

The finite element mesh is composed of axisymmetric elements with 4 nodes, 4 integration points, 2 displacement degrees of freedom (dof) and 1 temperature dof per node. The average element size of in the blank is 0.05mm (6 element through the thickness of 0.3mm). Larger elements are used in the tools.

The forces and displacements are applied on the blank holder, punch driver and ejector driver using rigid body tool drivers. Details about the applied forces and displacement are given in [3].

In order to consider the effect of rest of the machine press (missing parts, which is connected to the other steel parts) on the temperature distribution within the tools, conductive heat flux using a thin film, was employed.

$$q_{cond} = H_{cond}(T - T_{ref}) \quad (5)$$

With H_{cond} is the heat transfer coefficient and T_{ref} is a reference temperature, taken equal to (296.15K=23 °C) as the room temperature. H_{cond} is assumed to be equal to $1.5\ W/(m^2K)$.

When blank and tools come into contact, the heat is conducted using the following formula:

$$q_{contact} = H_{TC}(T_1 - T_2) \quad (6)$$

where, $q_{contact}$ is the conduction heat flux, H_{TC} is the conduction film coefficient between the two surfaces. It is assumed to be equal to $500\ W/(m^2K)$. T_1 is the surface temperature (K) in the blank and T_2 is the temperature in the tool at the same contact location.

The temperature increase in the tools is due to the conversion of plastic strain energy to heat in the blank, which is then transferred through contact, in addition to the heat generated from the contact shear energy (i.e. frictional heating) at the interface tools/blank.

Fig. 5 shows an example of the temperature increase during the deep drawing simulations.

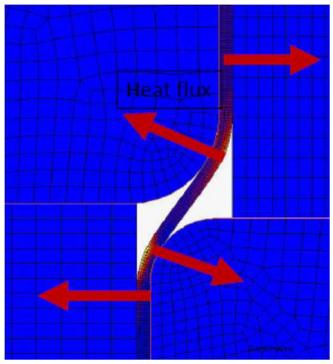

Fig. 5: The heat flux generated by plastic deformations and contact shear stresses from the blank to tools.

Materials behavior law: the material behavior of the blank is described by the a viscoplastic hardening model [4], with Hill'48 as a yield surface, to account for the normal anisotropy in the material. The used hardening behavior is shown in Equation 7. The first two terms represent the static hardening curve and the third the strain rate hardening contribution (Krabiell-Dahl). The Krabiell-Dahl term is additive to the static hardening curve, instead of the more usual multiplicative term.

$$\sigma_y(\bar{\varepsilon}) = \sigma_0 + \Delta\sigma_m\left[\beta(\bar{\varepsilon}+\varepsilon_0) + \left\{1 - e^{-\Omega(\bar{\varepsilon}+\varepsilon_0)}\right\}^n + \sigma_0^*\left[1 + \frac{kT}{\Delta G_0}\cdot\ln\left(\frac{\dot{\varepsilon}}{\dot{\varepsilon}_0}\right)\right]^m\right] \quad (7)$$

$\sigma_y(\bar{\varepsilon})$ is the isotropic hardening stress. $\bar{\varepsilon}$ is the equivalent plastic strain and $\dot{\varepsilon}$ is the equivalent strain rate, σ_0 is the initial yield stress. $\Delta\sigma_m$ is a parameter of work hardening scaling, ε_0 and $\dot{\varepsilon}_0$ are reference strain and reference strain rate, respectively, k is Boltzmann's constant. β, Ω, n, σ_0^*, ΔG_0, m are material parameters fitted using standard tests.

This hardening flow equation is implemented in MSC.Marc using a user subroutine.

The tools are modelled by simple linear elastic law, with a Young's modulus of 580 GPa and Poisson's coefficient of 0.23.

Contact friction model: traditionally, a constant value for the friction coefficient for deep drawing simulations is used. In the framework of the ASPECT project, a more advanced friction model from TriboForm [5] is used, based on the work of Hol et al. [6] using a multiscale approach. Local friction coefficients

are estimated based on the real surface topographies of tools through analytical expressions taking in the statistical surface parameters, considering lubricant amount (see Fig. 6). Asperity flattening under normal as well as tangential loading was included along with the local material flow near rough tool surfaces. The local information on friction coefficients are then supplied to a full-scale simulation of a deep drawing process.

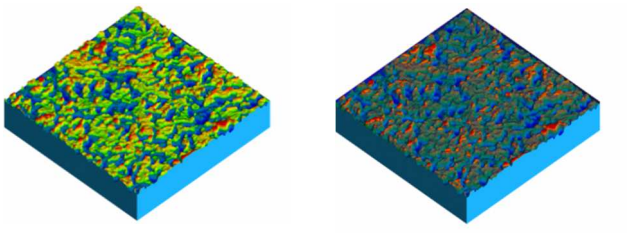

Fig. 6: Example of sheet surface topography with different lubrication amounts: (left) 0.6 g/m^2 (right) 2.0 g/m^2[7].

3.3. Implementation in MSC.Marc software

From an implementation point of view, we use the MSC.Marc model sections to extract the temperatures that are used for the polynomial fit of the 4D friction table, generated by TriboForm and jump in strokes approach using Taylor development. A model section is defined as a self-contained (part of a) finite element (FE) model, containing all the relevant FE information including material model and the full thermo-mechanical state (stresses, strains, temperatures, etc.). These sections files are saved to be used as initial conditions for the jump in strokes, as shown in the Fig. 7.

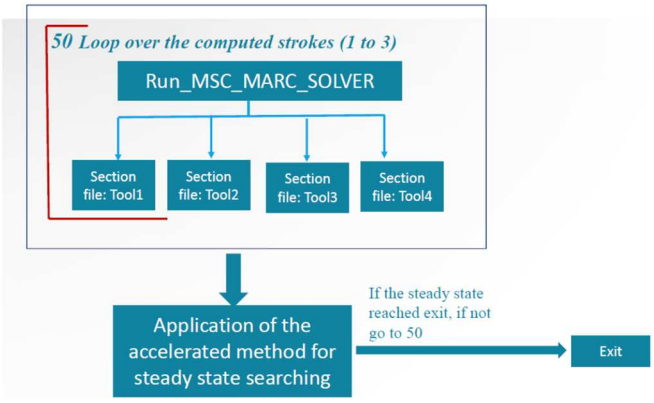

Fig. 7: Illustration of the implementation of the jump in stroke.

Fig. 8 shows the temperature predictions using the jump in strokes method compared to the result obtained by incremental method, for a testing case. The gained CPU time is around 60%, with very good predictions accuracy in this case.

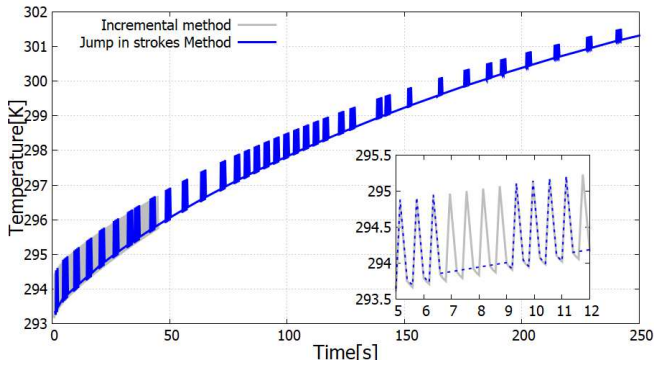

Fig. 8: Example of comparison between the temperature value obtained by incremental method and by jump in strokes method.

3.4. Experimental validation

In order to validate the proposed method experimentally, Thermocouples are placed on the dies for both step-1 and step-2, see highlighted regions in the Fig. 9.

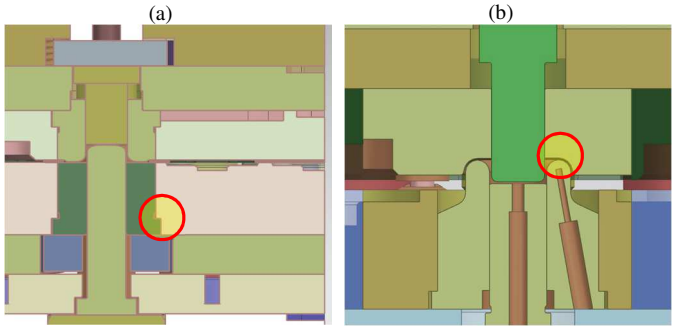

Fig. 9: The position of the thermocouples on the Dies for the two steps: (a) step-1, (b) step-2.

Fig. 10 shows the temperatures values measured by the two thermocouples during the process for a time of observation of 300 seconds. It also shows the predictions by the proposed method for the two steps. The estimated temperatures are in the range of the measured temperatures. Better correlation between the experimental measurement and the numerical predictions may be reached using further optimized boundary conditions, mainly the thermal ones.

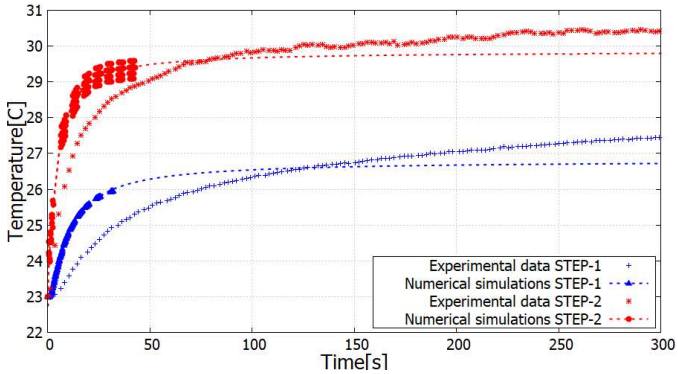

Fig. 10: Experimental die temperature for the two steps compared to numerical predictions using the jump in strokes method.

4. Application to automotive industry

4.1. The Opel use case

The spare wheel well of the Opel Insignia B is a double part produced from a hot dipped galvanized bake hardening steel (CR180B2) and is known as a part reacting sensitively on temperature changes during the production (see Fig. 11). The plastic deformation of the blank as well as the friction work between the tools and the metal sheet is leading to a quick heating of the tools resulting in an increased friction coefficient, which is causing part failure due to higher restraining forces.

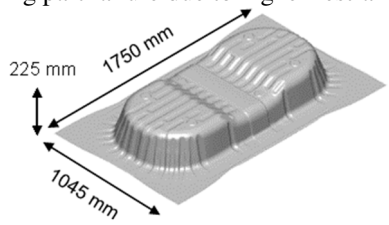

Fig. 11: Deep drawing operation of the Opel use case

4.2. The finite element model for a single stroke

Thermo-mechanical modelling: to capture the effect of temperature on the formability of the deep drawn part, a thermal-mechanical coupled simulation is created within the ESI PAM-STAMP software. The mechanical and transient thermal problems are solved by an explicit time integration scheme. Shell elements of type Belytschko-Tsay with 5 integration points over the thickness are used to mesh the blank. The tools are rigid, only their thermal evolution is considered. For thermo-mechanical simulations in which cooling channels are considered, the state of the art prescribes to use a volumetric tool mesh. Meanwhile the gradient temperature inside the tool can be neglected and the relevant quantity is the surface temperature, which is the input of the frictional model. In this case a 2D thermal shell element (see Fig. 12) is used to model the heating up in the tools.

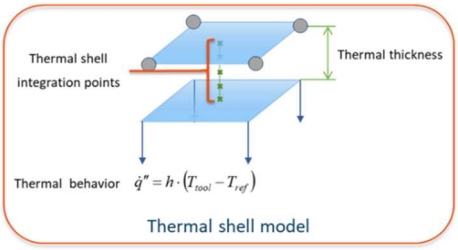

Fig. 12: Thermal shell model for tools.

The two key parameters, the thermal thickness (5.853 mm) and the convection coefficient h (1081.31 $W.m^{-2}K^{-1}$) have been calibrated using an inverse parameters identification method with ESI PAM-OPT [2] by comparing numerical results linked to a volumetric model and thick shell element of the same surface dimensions. The 2 sources of heat in the tools which are the heat converted from the plastic strain in the blank (modelled by Taylor-Quinney equation [8]) and the friction between the blank and the tools are considered in these simulations.

Mechanical and thermal properties: the simulation uses a strain-rate dependent hardening curve and a Vegter Standard yield locus as well as a forming limit curve (FLC) determined by Nakazima tests [9]. Since simulations including a temperature dependency of the hardening curve have not shown any effect on the formability of the deep drawn part considering temperatures of up to 100 °C, the temperature dependent material behavior will be neglected. The thermal properties used for the tools and the blank have been derived from the material specifications of the suppliers and are summarized in Table 1.

Table 1: Thermal properties of the finite element model (Opel use case)

Parameter	**Tools (GGG70L)**	**Blank (CR180B2)**
Conductivity	31.1 W/mK	50 W/mK
Specific heat	460 J/kgK	460 J/kgK
Thermal thickness	5.85 mm	-
Planar conduct. factor	0.1	-
Dissipation factor	-	0.9
Surface heat transfer coeff. (see Fig. 13)	f(gap), f(pressure)	f(gap), f(pressure)

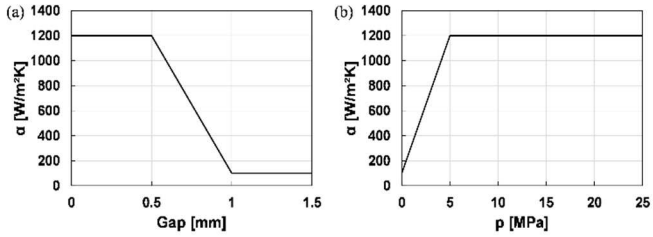

Fig. 13: Variable heat transfer coefficient function of gap (a) and pressure (b) derived from [10][11][12].

Contact and friction modelling: a nonlinear penalty formulation is used to model the contact and the heating of the contact interface by dissipation of friction work is considered by a surface heat flux applied to the contact facing outer fiber of the shell elements:

$$\dot{q} = \beta \cdot \mu \cdot \sigma_n \cdot |v_{rel}| \tag{8}$$

where β is the partitioning factor set to 0.5 to assure an equal distribution of the heat between the blank and the tools both steels; $\mu \cdot \sigma_n \cdot |v_{rel}|$ is the generated friction power with μ the friction coefficient. A basic constant Coulomb model could not model the tribological changes due to temperature increase and so the impact on the mechanical formability of the part. That's why a temperature, velocity and pressure dependent friction model has been implemented by using a user subroutine. For this purpose, experimental data from strip drawing tests, performed by Filzek TRIBOtech company, have been approximated based on the least squares method using a friction model from Hora et al. (see equation 9) [13].

$$\mu(p, v, T) = A \cdot (p_0 + p)^{-a} \cdot \left(\frac{(T+273)-T_0}{T_0}\right)^{b} \cdot (v_0 + v)^{-c} \tag{9}$$

An excerpt of the experimental data including the approximation

by the friction model for the tribological system of the Opel use case can be seen in Fig. 14a. As expected, an increasing tool temperature is leading to a higher friction level, whereas the friction coefficient is decreasing with higher surface pressures.

To consider parameters with subject to stochastic fluctuations of the tribological system as well, several offline measurements have been carried out for the application example. The distribution of the lubrication amount on the surface of the blank as well as the tool surface roughness and the blank surface roughness have been considered as main influences on the tribological system. Since the measurements have not shown significant deviations of the tool and blank surface roughness, they are assumed to be constant within the finite element model. However, the distribution of the lubrication amount is inhomogeneous with a lower amount in the middle of the blank compared to the outside of the blank, which is a result from the rolling process and can be expected for most coil lubrications. The great impact of the lubrication amount on the friction behavior is taken into account by different friction models considering different lubrication amounts. Fig. 14b shows the corresponding approach for the simulation in which we used a tailored blank approach to consider these variations.

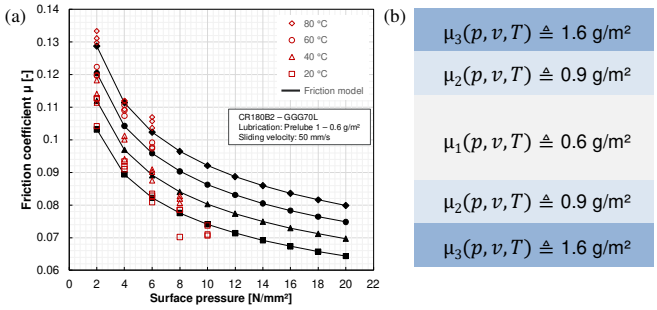

Fig. 14: Excerpt of the experimental data from strip drawing tests (a) and varying friction models based on different lubrication amounts (b).

4.3. Implementation and validation in ESI PAM-STAMP software

The global Jump in stroke algorithm is represented in Fig. 15. It contains the incremental algorithm which deals with the automation of the launching of multiples FE simulations under the stamping software. It allows to transfer the thermal history of tool nodes between each computation and launch the FE simulations automatically. The convergence towards the steady state is controlled by a stopping criterion which is either a precision required or a maximal number of strokes. The 2nd part is the reduction of the number of simulations, being the jump in strokes method. In the same way than for the incremental algorithm, between each series of incremental strokes, the extrapolated temperature field is recovered and transferred as input data for the new series of strokes.

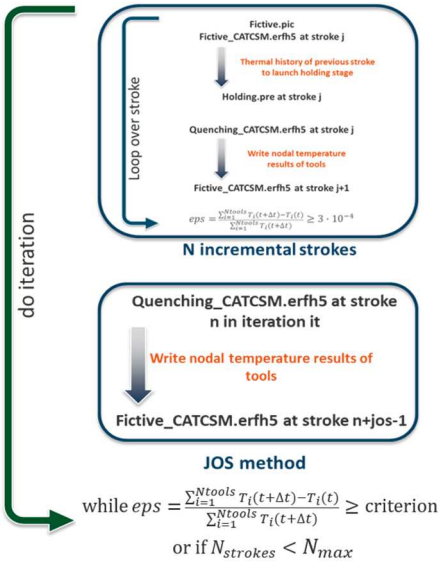

Fig. 15: Algorithm of the global strategy of Jump in strokes method.

In order to validate the method and its implementation, a simple study case has been considered: the stamping of a square cup (see Fig. 16).

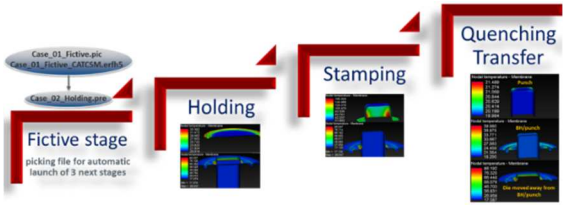

Fig. 16: Square cup, stages of the process.

The thermo-mechanical simulation contains the holding, the stamping and the quenching phases. The last stage allows to model the time between 2 parts stamped and during which the tools cool down. The validation has been done purely numerically comparing the 2 methods, incremental and jump in strokes. The results of a node located on the drawbeads of the blankholder (see Fig. 17) show a good approximation of the acceleration method (see Fig. 18). The error of the jump in strokes method with respect to the incremental one is very small (see Table 2). The method allowed a saving in the total CPU time of a factor 2 to 3 for an approximation error less than 0.3%.

Fig. 17: Node 21851 located on the drawbeads.

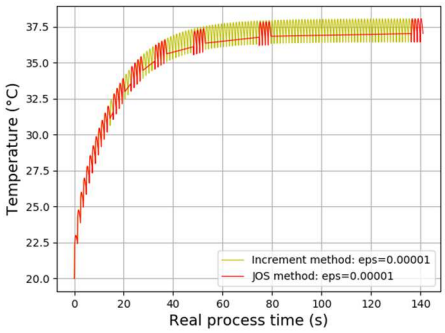

Fig. 18: Temperature of the node 21851 over all strokes for incremental method (yellow) and jump in strokes (red) for steady state criterion = $1 \cdot 10^{-5}$.

Table 2. Comparison incremental / JOS method: Square cup case, temperature in the node 21851 for two different steady criteria.

		$eps = 2 \cdot 10^{-4}$		$eps = 1 \cdot 10^{-5}$	
		Incremental	JOS	Incremental	JOS
Strokes number		66	32	115	36
T(°C) Node 21851:	min	36.32	36.23	36.43	36.44
	max	37.94	37.85	38.05	38.06
Error on (%)	min		0.24		0.01
	max		0.23		0.01

4.4. Experimental validation

Experimental measures of temperature have been done at Opel in some locations of the blankholder and the punch (see Fig. 19).

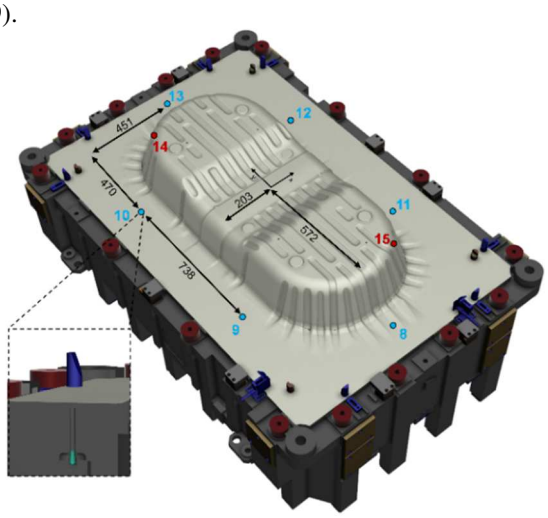

Fig. 19: Pyrometers located in the blank holder (blue) and the punch (red) of the Opel tools.

The thermal state in the tools and the blank at initial state and after reaching the steady state is visible on the Fig. 20. A comparison has been done between experimental and numerical results. For example, sensor 10 reach maximal values of 41.5 °C and numerical results show an increase until 40 °C when steady state is reached (see Fig. 21). The results are in the range of the temperature measured. Some data, such as the quenching step and heat exchange coefficients need to be adjusted to improve the fit with experimental temperature data.

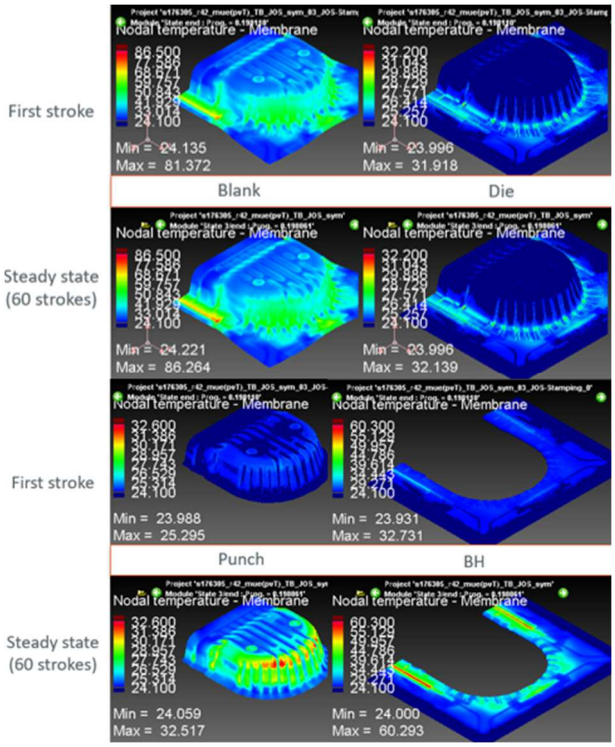

Fig. 20: Thermal results in the tools and the blank at 1st and 60th stroke.

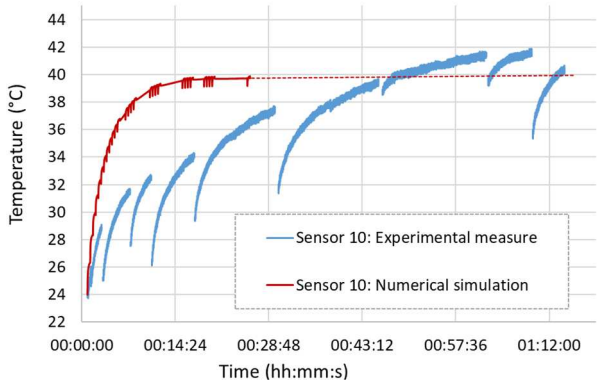

Fig. 21: Experimental and numerical temperature evolution of sensor 10.

If we impose an initial homogeneous temperature on the tools of 60 °C (see Fig. 22), we can see that thinning is higher and that cracks appears. Considering a pressure, velocity, temperature dependent friction, allows to consider an impact on formability. However, this assumption of homogeneous tool temperatures is not representative of the reality and the maximal temperatures are not known. The jump in strokes strategy is applied to have a better accuracy of the temperature increase. However, for the current case, no significant impact on mechanical aspect is currently observed. Indeed, the friction model has been calibrated considering input data not enough representative of the real tool from Opel and so this friction model is not enough sensitive to temperature increase. New friction tests are being done considering more realistic data like the lubricant amount and the tool roughness of the Opel demonstrator. A study with the TriboForm model will also be done.

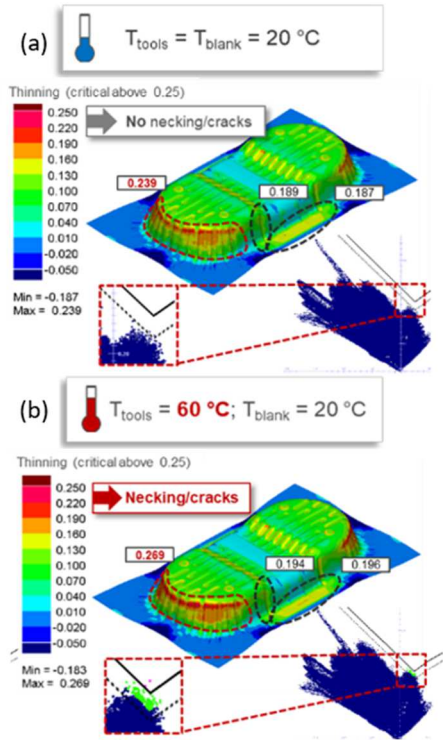

Fig. 22: Comparison of thinning and cracks between homogeneous tools, at 20 °C (a) and 60 °C (b).

5. Conclusion

In this work a speed-up method called "Jump in strokes method" was proposed and implemented within two FEM software packages, being MSC.Marc and ESI PAM-STAMP. The accuracy of the method was checked against the incremental method, which showed the potential of the method. The method was also used to model two challenging use-cases at different scales: small parts used for consumer goods proposed by Philips and large ones used for cars industry proposed by Opel. Experimental measurements were performed during the industrial runs for the two processes and compared to the corresponding FE models predictions together with the Jump in stroke method. The validity of the numerical predictions is related to the accuracy of the assumptions and approaches considered in each single stroke FE models, such as modeling of the friction behavior and the definition of the thermal boundary conditions.

New friction tests considering more accurately the tribological conditions of the process may allow to better model the impact of the temperature increase on the formability. Quenching properties and thermal exchanges coefficients also need to be adjusted to fit more precisely with the heating up of the real tools.

The jump in strokes method allowed in both cases to reduce considerably the total CPU time up to 60% and simulating the processes until steady state with a good accuracy. It would be a suitable tool to simulate complex behaviors occurring due to the start-up effect such as defects in forming processes related to the increase of temperature in the tools.

Acknowledgements

This research was carried out within the project "ASPECT – Advanced Simulation and control of tribology in metal forming Processes for the North-West European Consumer goods and Transport sectors" (project number NWE 220), co-funded by the INTERREG North West Europe program www.nweurope.eu/aspect

References

[1] Cojocaru D, Karlsson A. A simple numerical method of cycle jumps for cyclically loaded structures. International Journal of Fatigue 2006; 28: 1677–1689.
[2] www.esi-group.com.
[3] Veldhuis M, Heingärtner J, Krairi A, Waanders D, Hazrati J. An Industrial-Scale Cold Forming Process Highly Sensitive To Temperature Induced Frictional Start-up Effects To Validate A Physical Based Friction Model. 23rd International Conference on Material Forming (ESAFORM 2020).
[4] Vegter H, Mulder H, van Liempt P, Heijne J. Work hardening descriptions in simulation of sheet metal forming tailored to material type and processing, International Journal of Plasticity 2006; 80: 204-221.
[5] Waanders D, Hazrati Marangalou J, Hol J. Temperature Dependent Friction Modelling: The Influence Of Temperature On Product Quality. 23rd International Conference on Material Forming (ESAFORM 2020).
[6] Hol J, Meinders T, Huetink J, Menary G. A multi-scale friction model framework for full scale sheet forming simulations. International Journal for Quality in Health Care 2011; 1353: 207-212.
[7] www.triboform.com
[8] Taylor GI, Quinney H. The plastic distortion of metals. Pilos. Trans. Roy. Soc., London, A230, London; 1931.
[9] Atzema E, Mulder H. Temperature Dependence of Steel Constitutive Behavior: A Simplified Model. 23rd International Conference on Material Forming (ESAFORM 2020).
[10] Kim H, Altan T, Yan Q. Evaluation of stamping lubricants in forming advanced high strength steels (AHSS) using deep drawing and ironing tests. Journal of Materials Processing Technology 2009; 209(8): 4122-4133.
[11] Schmid P, Liewald M. Experimental Determination of Heat Transfer Coefficients for Forming of Stainless Steel Sheets Considering Process Conditions and Deep-Drawing Film. In Key Engineering Materials 2013. 554: 1501-1508. Trans Tech Publications.
[12] Altan T, Tekkaya AE. Sheet metal forming: processes and applications. ASM international Eds 2012.
[13] Hora P, Heingärtner J, Manopulo N, Tong L. Applicability of cognitive systems, metamodels and virtual tools for an in-line of process robustness control. In T&F Conference "Tools and Technologies for Processing Ultra High Strength Materials" 2011. The European Institute Tools & Forming.